Some closed form series solutions to peridynamic plate equations

Zhenghao Yang[a], Konstantin Naumenko[b,*], Chien-Ching Ma[a], Holm Altenbach[b], Erkan Oterkus[c], Selda Oterkus[c]

[a]*Department of Mechanical Engineering, National Taiwan University, Taipei, Taiwan*
[b]*Otto-von-Guericke-University Magdeburg, Institute of Mechanics, PF 4120, 39016, Magdeburg, Germany*
[c]*PeriDynamics Research Centre, Department of Naval Architecture, Ocean and Marine Engineering, University of Strathclyde, Glasgow, United Kingdom*

Abstract

Peridynamics is a generalized continuum theory which is developed to account for long range internal force/moment interactions. Peridynamic equations of motion are of integro-differential type and only several closed-form analytical solutions are available for elementary structures. The aim of this paper is to derive analytical solutions to peridynamic Kirchhoff type (shear rigid) plates equations for both static and dynamic cases. Applying trigonometric series with respect to in-plane coordinates, solutions for the deflection function of a rectangular simply supported plate are derived. The coefficients in the series are presented in a closed analytical form such that the equations of motion are exactly satisfied. For the dynamic case the solution is derived applying the variable separation with respect to the time and the in-plane coordinates. Several numerical cases are presented to illustrate the derived solutions. Furthermore, results of peridynamic plate equations are compared against results obtained from the classical plate theory. A very good agreement between these two theories is obtained for the case of the small horizon sizes which shows the capability of the presented approach.

Keywords: Peridynamics, plate theory, analytical solution, rectangular plate

1. Introduction

Peridynamics (PD) is a generalized continuum theory which accounts for long-range force/moment interactions [1]. Unlike the classical continuum mechanics (CCM) and classical structural mechanics theories of beams, plates and shells, the deformation gradient, its higher gradients or gradients of state variables are not introduced in PD. PD equations of motion are of integro-differential type, in contrast to CCM where partial differential equations are derived. This makes PD attractive in modeling fracture processes such as crack initiation [2] and crack branching [3].

Peridynamic formulations for elementary structures including rods and beams [4], plates [5–7] and shells [8, 9] are available. Within the CCM these theories provide an efficient and robust approach for the structural analysis. Indeed many closed form and/or approximate analytical solutions based on the classical theories of plates and shells are derived in the literature, e.g. in [10, 11] and provide a direct insight into the deformation

*Corresponding author

Email addresses: zhenghao.yang@strath.ac.uk (Zhenghao Yang), konstantin.naumenko@ovgu.de (Konstantin Naumenko), ccma@ntu.edu.tw (Chien-Ching Ma), holm.altenbach@ovgu.de (Holm Altenbach), erkan.oterkus@strath.ac.uk (Erkan Oterkus), selda.oterkus@strath.ac.uk (Selda Oterkus)

and stress states. Furthermore, analytical solutions were mostly applied to validate general purpose numerical methods, such as the finite element method and to analyze the accuracy of numerical solutions. However, within the framework of PD only few analytical solutions are available. For one-dimensional rods in both peristatic and peridynamic cases analytical solutions are derived in [12–14].
The aim of this study is to derive analytical solutions to PD Kirchhoff-type (shear-rigid) plate equations for both static and dynamic loading conditions. By use of double trigonometric series representation, general solutions for the deflection function with respect to the in-plane coordinates are presented. For simply supported rectangular plates the coefficients in the series are given in a closed analytical form. The results are validated by comparing against solutions to the classical plate theory (CPT) for both static and dynamic cases.

2. Peridynamic plate theory

According to the Kirchhoff (shear-rigid) plate theory the displacement field is expressed as follows [10]

$$\mathbf{u}(\mathbf{x}, z) = \boldsymbol{\varphi}(\mathbf{x})z, \quad \boldsymbol{\varphi} = -\boldsymbol{\nabla} w, \quad w\,(\mathbf{x}, z) = w\,(\mathbf{x}) \tag{1}$$

where $\mathbf{u} = u_i \mathbf{e}_i$, $i = 1, 2$ is the in-plane displacement vector, $\boldsymbol{\varphi} = \varphi_i \mathbf{e}_i$ is the cross-sectional rotation vector and w is the deflection. $\mathbf{x} = \mathbf{e}_i x_i$ is the in-plane position vector, $x_1 = x$, $x_2 = y$ are in-plane Cartesian coordinates and $\mathbf{e}_i$ are the corresponding base vectors. z is the transverse coordinate, $-h/2 \le z \le h/2$ with h being the plate thickness. $\boldsymbol{\nabla} = \mathbf{e}_i \frac{\partial}{\partial x_i}$ is the nabla (Hamilton) operator. Here and in the sequel the summation over repeated indices is applied. With Eq. (1) and the elasticity law, the linear strain tensor $\boldsymbol{\varepsilon}$, the curvature tensor $\boldsymbol{\kappa}$ and the Cauchy stress tensor $\boldsymbol{\sigma}$ are computed as follows

$$\boldsymbol{\varepsilon}(\mathbf{x}, z) = \boldsymbol{\kappa}(\mathbf{x})z, \quad \boldsymbol{\kappa} = -\boldsymbol{\nabla}\boldsymbol{\nabla} w, \quad \boldsymbol{\sigma} = \frac{Ez}{1-\nu^2}\left[(1-\nu)\boldsymbol{\kappa} + \nu \mathrm{tr}\,\boldsymbol{\kappa}\boldsymbol{P}\right], \tag{2}$$

where E is the Young modulus, ν is the Poisson ratio and $\mathbf{P} = \mathbf{e}_i \otimes \mathbf{e}_i$ is the projector. The strain energy per unit area can be written as follows

$$W = \frac{D}{2}\left[(1-\nu)\left(\mathrm{tr}\,(\boldsymbol{\kappa}^2) - (\mathrm{tr}\,\boldsymbol{\kappa})^2\right) + (\mathrm{tr}\,\boldsymbol{\kappa})^2\right], \quad D = \frac{Eh^3}{12(1-\nu^2)} \tag{3}$$

Let A be the plate midplane area with piecewise-smooth boundary Γ. With the identity

$$\mathrm{tr}\,(\boldsymbol{\kappa}^2) = (\mathrm{tr}\,\boldsymbol{\kappa})^2 - \boldsymbol{\nabla} \cdot [(\boldsymbol{\kappa} - \mathrm{tr}\,\boldsymbol{\kappa}\mathbf{P}) \cdot \boldsymbol{\nabla} w] \tag{4}$$

and by integration the total strain energy U stored in the plate is computed by

$$U = \int\limits_A W dA = \int\limits_A \frac{D}{2}(\mathrm{tr}\,\boldsymbol{\kappa})^2\, dA - \frac{D}{2}(1-\nu)\oint\limits_\Gamma \boldsymbol{\upsilon} \cdot (\boldsymbol{\kappa} - \mathrm{tr}\,\boldsymbol{\kappa}\mathbf{P}) \cdot \boldsymbol{\nabla} w ds, \tag{5}$$

where $\boldsymbol{\upsilon}$ is the unit normal at points to the smooth parts of the boundary Γ and s is the arc length coordinate. The boundary integral in (5) can be represented as follows

$$\oint\limits_\Gamma \boldsymbol{\upsilon} \cdot (\boldsymbol{\kappa} - \mathrm{tr}\,\boldsymbol{\kappa}\mathbf{P}) \cdot \boldsymbol{\nabla} w ds = \oint\limits_\Gamma \left[w_{,\tau\tau}\, w_{,\upsilon} - w_{,\upsilon\tau}\, w_{,\tau} + k(w_{,\upsilon})^2\right] ds, \tag{6}$$

where $w_{,\upsilon}$ and $w_{,\tau}$ are derivatives of the deflection with respect to the normal and tangential directions, respectively and k is the curvature at points of the smooth part of Γ. For plates with clamped edges $w = 0$,

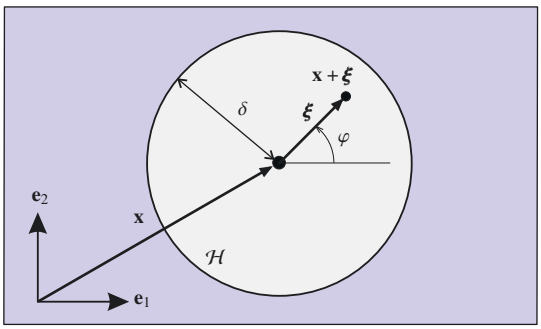

Fig. 1. Finite neighborhood around material point **x** with horizon δ

$w_{,\upsilon} = 0$, $w_{,\tau} = 0$, and the boundary integral (6) takes zero value. For simply supported plates $w = 0$ and $w_{,\tau} = 0$, and the boundary integral vanishes only for straight boundaries with $k = 0$. In these cases Eq. (5) can be reduced to

$$U = \int_A \frac{D}{2} \left(\operatorname{tr} \boldsymbol{\kappa}\right)^2 dA = \int_A \frac{D}{2} \left(\Delta w\right)^2 dA, \tag{7}$$

where Δ is the Laplace operator. The corresponding total strain energy function in PD theory can be obtained by converting each local term in Eq. (7) into the equivalent nonlocal form. Performing Taylor expansion for deflection function $w(\mathbf{x})$ about material point $\mathbf{x}$ and ignoring higher order terms yields

$$w\left(\mathbf{x}+\boldsymbol{\xi}\right) - w\left(\mathbf{x}\right) = \boldsymbol{\xi} \cdot \boldsymbol{\nabla} w|_{\mathbf{x}} + \frac{1}{2}\, \boldsymbol{\xi} \otimes \boldsymbol{\xi} \cdot\cdot\, \boldsymbol{\nabla}\boldsymbol{\nabla} w|_{\mathbf{x}}\,, \tag{8}$$

where $\boldsymbol{\xi}$ is is the bond vector between two interacting material points in the plate plane within a finite neighborhood $\mathcal{H}$ of the material point $\mathbf{x}$, as illustrated in Fig. 1. Dividing each term of Eq. (8) by $\xi^2 = \boldsymbol{\xi} \cdot \boldsymbol{\xi}$ and integrating over $\mathcal{H}$ yields the following Eqs

$$\int_{\mathcal{H}} \frac{w(\mathbf{x}+\boldsymbol{\xi}) - w(\mathbf{x})}{\xi^2} dA_{\boldsymbol{\xi}} = \frac{1}{2} \int_{\mathcal{H}} \mathbf{N}\, dA_{\boldsymbol{\xi}} \cdot\cdot\, \boldsymbol{\nabla}\boldsymbol{\nabla} w, \quad \int_{\mathcal{H}} \frac{w(\mathbf{x}+\boldsymbol{\xi}) - w(\mathbf{x})}{\xi^2} \mathbf{N} dA_{\boldsymbol{\xi}} = \frac{1}{2} \int_{\mathcal{H}} \mathbf{N} \otimes \mathbf{N}\, dA_{\boldsymbol{\xi}} \cdot\cdot\, \boldsymbol{\nabla}\boldsymbol{\nabla} w, \tag{9}$$

where

$$\mathbf{N} = \mathbf{n} \otimes \mathbf{n}, \quad \xi = |\boldsymbol{\xi}|, \quad \mathbf{n} = \frac{\boldsymbol{\xi}}{\xi}, \quad \mathbf{n} = \cos\varphi \mathbf{e}_1 + \sin\varphi \mathbf{e}_2$$

By integration we obtain

$$\int_{\mathcal{H}} \mathbf{N}\, dA_{\boldsymbol{\xi}} = \frac{\pi\delta^2}{2} \mathbf{P}, \quad \int_{\mathcal{H}} \mathbf{N} \otimes \mathbf{N}\, dA_{\boldsymbol{\xi}} = \frac{\pi\delta^2}{4} \left(\mathbf{P} \otimes \mathbf{P} + \mathbf{e}_i \otimes \mathbf{P} \otimes \mathbf{e}_i + \mathbf{e}_i \otimes \mathbf{e}_k \otimes \mathbf{e}_i \otimes \mathbf{e}_k\right) \tag{10}$$

From Eqs (9) and (10) the PD curvature tensor and its first invariant are computed as follows

$$\bar{\boldsymbol{\kappa}} = -\frac{2}{\pi\delta^2} \int_{\mathcal{H}} \frac{w(\mathbf{x}+\boldsymbol{\xi}) - w(\mathbf{x})}{\xi^2} \left(4\mathbf{N} - \mathbf{P}\right) dA_{\boldsymbol{\xi}}, \quad \operatorname{tr} \bar{\boldsymbol{\kappa}} = -\frac{4}{\pi\delta^2} \int_{\mathcal{H}} \frac{w(\mathbf{x}+\boldsymbol{\xi}) - w(\mathbf{x})}{\xi^2} dA_{\boldsymbol{\xi}} \tag{11}$$

A class of PD theories of elastic plates can be derived assuming the correspondence of the strain energy density from the classical theory defined as a function of the PD deformation measures and the PD strain

energy density [7]. Applied for the Kirchhoff plates this correspondence leads to the following peridynamic strain energy density $\bar{U}$

$$\bar{U}(w'-w) = U(\bar{\boldsymbol{\kappa}}) = \frac{D}{2}\int\limits_A \left[(1-\nu)\left(\mathrm{tr}\,(\bar{\boldsymbol{\kappa}}^2) - (\mathrm{tr}\,\bar{\boldsymbol{\kappa}})^2\right) + (\mathrm{tr}\,\bar{\boldsymbol{\kappa}})^2\right] dA, \tag{12}$$

where $w' = w(\mathbf{x}+\boldsymbol{\xi})$ and the non-local curvature tensor is defined by Eq. (11). For plates with simply supported and/or clamped edges the reduced form of the strain energy density (7) can be applied providing the following PD strain energy density

$$\bar{U}(w'-w) = U(\bar{\boldsymbol{\kappa}}) = \frac{D}{2}\int\limits_A (\mathrm{tr}\,\bar{\boldsymbol{\kappa}})^2 dA = \frac{D}{2}\left(\frac{4}{\pi\delta^2}\right)^2 \int\limits_A \left(\int\limits_{\mathcal{H}} \frac{w(\mathbf{x}+\boldsymbol{\xi}) - w(\mathbf{x})}{\xi^2} dA_{\boldsymbol{\xi}}\right)^2 dA \tag{13}$$

The PD equation of motion can be derived by using the following Lagrange's equation

$$\frac{d}{dt}\frac{\partial K}{\partial \dot{w}} = -\frac{\partial \Pi}{\partial w}, \quad K = \frac{1}{2}\int\limits_A \rho h \dot{w}^2(\mathbf{x}) dA, \quad \Pi = \bar{U} - \int\limits_A p(\mathbf{x}) w(\mathbf{x}) dA, \tag{14}$$

where K is the kinetic energy and Π is the potential energy and p is the given distributed lateral load. For plates with simply supported and/or clamped edges Eqs (13) and (14) yield

$$\rho h \ddot{w} = c\int\limits_{\mathcal{H}} \frac{1}{\xi^2}\left[\int\limits_{\mathcal{H}}\left(\frac{w(\mathbf{x}+\boldsymbol{\eta}) - w(\mathbf{x})}{\eta^2}\right) dA_{\boldsymbol{\eta}} - \int\limits_{\mathcal{H}}\left(\frac{w(\mathbf{x}+\boldsymbol{\xi}+\boldsymbol{\eta}) - w(\mathbf{x}+\boldsymbol{\xi})}{\eta^2}\right) dA_{\boldsymbol{\eta}}\right] dA_{\boldsymbol{\xi}}, \quad c = \left(\frac{4}{\pi\delta^2}\right)^2 D \tag{15}$$

3. Boundary conditions

Note that Eq. (15) holds only if the PD horizon of material point is completely accommodated within the plate. For material points adjacent to the boundary whose PD horizon is incomplete within the body, it is necessary to introduce fictitious region outside the boundary as shown in Fig. 2. In this study the width of the fictitious region is suggested to be twice the PD horizon size, 2δ, and the displacement field of the fictitious region is forced to be anti-symmetric with respect to the real region as explained below. Suppose a rectangular plate subjected to simply supported boundary condition with origin allocated at left corner, from geometric point of view, the edge $x = 0$ satisfies the following conditions

$$w\,(0,y) = 0, \quad \kappa_x\,(0,y) = \left.\frac{\partial^2 w}{\partial x^2}\right|_{(0,y)} = 0 \tag{16}$$

Applying the central difference scheme on Eq. $(16)_2$ and associating with Eq. $(16)_1$ gives

$$\frac{1}{\xi^2}[w(-\xi,y) - 2w(0,y) + w(\xi,y)] = 0, \quad \Rightarrow \quad w\,(-\xi,y) = -w\,(\xi,y) \tag{17}$$

Likewise, other three edges satisfy the following

$$w\,(a+\xi,y) = -w\,(a-\xi,y), \quad w\,(x,-\xi) = -w\,(x,\xi), \quad w\,(x,b+\xi) = -w\,(x,b-\xi) \tag{18}$$

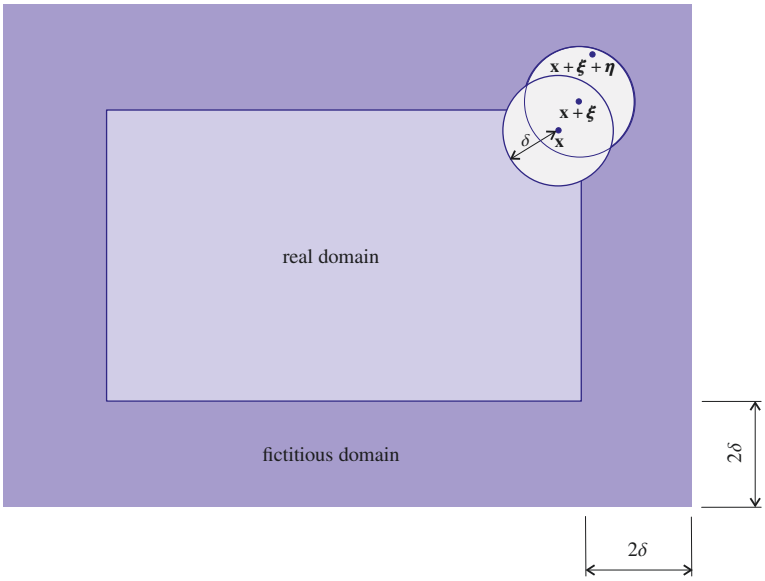

Fig. 2. Real and fictitious domains for the plate

4. Peristatic solution

Consider a simply supported plate, with the length a and width b, subjected to arbitrary distributed load $p\,(x, y)$. The PD governing equation follows from Eq. (15)

$$c\int_0^{2\pi}\int_0^{\delta}\frac{1}{\xi}\left[\begin{array}{l}\displaystyle\int_0^{2\pi}\int_0^{\delta}\frac{w\,(x+\eta_1, y+\eta_2)-w\,(x, y)}{\eta}d\eta d\theta \\ \displaystyle-\int_0^{2\pi}\int_0^{\delta}\frac{w\,(x+\xi_1+\eta_1, y+\xi_2+\eta_2)-w\,(x+\xi_1, y+\xi_2)}{\eta}d\eta d\theta\end{array}\right]d\xi d\varphi + p\,(x, y) = 0, \tag{19}$$

with $\eta_1 = \eta\cos\theta$, $\eta_2 = \eta\sin\theta$, $\xi_1 = \xi\cos\varphi$, $\xi_2 = \xi\sin\varphi$ and the boundary conditions (17) and (18). For the considered plate the displacement field can be represented as double Fourier sine series as follows

$$w\,(x, y) = \sum_{m=1}^{\infty}\sum_{n=1}^{\infty}A_{mn}\sin\frac{m\pi x}{a}\sin\frac{n\pi y}{b} \tag{20}$$

By utilizing Eq. (20), Eq (19) yields

$$c\sum_{m=1}^{\infty}\sum_{n=1}^{\infty}A_{mn}\sin\frac{m\pi x}{a}\sin\frac{n\pi y}{b}\left[\int_0^{2\pi}\int_0^{\delta}\frac{1}{\xi}\left(1-\cos\frac{m\pi\xi_1}{a}\cos\frac{n\pi\xi_2}{b}\right)d\xi d\varphi\right]^2 = p\,(x, y) \tag{21}$$

The undetermined coefficients A_{mn} can be casted by utilizing the orthogonality. As a result Eq. (20) gives the following analytical PD solution for simply supported Kirchhoff plates

$$w\left(x,y\right)=\sum_{m=1}^{\infty}\sum_{n=1}^{\infty}\frac{4}{ab}\frac{1}{c}\frac{\int_0^a\int_0^b p\left(x,y\right)\sin\frac{m\pi x}{a}\sin\frac{n\pi y}{b}dxdy}{\left[\int_0^{2\pi}\int_0^{\delta}\frac{1}{\xi}\left(1-\cos\frac{m\pi\xi_1}{a}\cos\frac{n\pi\xi_2}{b}\right)d\xi d\varphi\right]^2}\sin\frac{m\pi x}{a}\sin\frac{n\pi y}{b} \tag{22}$$

5. Peridynamic solution

The PD equation of motion for free vibrational problem can be derived from Eq. 15 as follows

$$\rho h\ddot{w}(x,y,t)=c\int_0^{2\pi}\int_0^{\delta}\frac{1}{\xi}\left[\begin{array}{l}\int_0^{2\pi}\int_0^{\delta}\frac{w\left(x+\eta_1,y+\eta_2,t\right)-w\left(x,y,t\right)}{\eta}d\eta d\theta\\ -\int_0^{2\pi}\int_0^{\delta}\frac{w\left(x+\xi_1+\eta_1,y+\xi_2+\eta_2,t\right)-w\left(x+\xi_1,y+\xi_2,t\right)}{\eta}d\eta d\theta\end{array}\right]d\xi d\varphi \tag{23}$$

with boundary conditions the boundary conditions (17) and (18) as well as initial conditions

$$w\left(x,y,0\right)=f\left(x,y\right),\quad \dot{w}\left(x,y,0\right)=g\left(x,y\right) \tag{24}$$

For a rectangular domain, the displacement function can be decomposed as

$$w\left(x,y,t\right)=\omega\left(x,y\right)T\left(t\right) \tag{25}$$

Plugging (25) into (23) and isolating the variables yields

$$\frac{\rho h}{c}\frac{\ddot{T}(t)}{T(t)}=\frac{1}{\omega(x,y)}\int_0^{2\pi}\int_0^{\delta}\frac{1}{\xi}\left[\begin{array}{l}\int_0^{2\pi}\int_0^{\delta}\frac{\omega(x+\eta_1,y+\eta_2)-\omega(x,y)}{\eta}d\eta d\theta-\\ \int_0^{2\pi}\int_0^{\delta}\frac{\omega(x+\xi_1+\eta_1,y+\xi_2+\eta_2)-\omega(x+\xi_1,y+\xi_2)}{\eta}d\eta d\theta\end{array}\right]d\xi d\varphi=-\lambda \tag{26}$$

which provides the characteristic functions

$$\int_0^{2\pi}\int_0^{\delta}\frac{1}{\xi}\left[\begin{array}{l}\int_0^{2\pi}\int_0^{\delta}\frac{\omega\left(x+\eta_1,y+\eta_2\right)-\omega\left(x,y\right)}{\eta}d\eta d\theta-\\ \int_0^{2\pi}\int_0^{\delta}\frac{\omega\left(x+\xi_1+\eta_1,y+\xi_2+\eta_2\right)-\omega\left(x+\xi_1,y+\xi_2\right)}{\eta}d\eta d\theta\end{array}\right]d\xi d\varphi+\lambda\omega\left(x,y\right)=0 \tag{27}$$

$$\frac{\rho}{c}\ddot{T}\left(t\right)+\lambda T\left(t\right)=0 \tag{28}$$

If we analogue $\omega(x,y)$ to $w(x,y)$ and $\lambda\omega(x,y)$ to $\frac{p(x,y)}{c}$ in Eqs (27) and (19), the trial function is

$$\omega(x,y) = \sum_{m=1}^{\infty}\sum_{n=1}^{\infty} B_{mn} \sin\frac{m\pi x}{a} \sin\frac{n\pi y}{b} \tag{29}$$

From Eq. (27) we obtain

$$\lambda_{mn} = \left[\int_0^{2\pi}\int_0^{\delta} \frac{1}{\xi}\left(1 - \cos\frac{m\pi\xi_1}{a}\cos\frac{n\pi\xi_2}{b}\right) d\xi d\varphi\right]^2 \tag{30}$$

The second characteristic function (28) has the general solution of the form

$$T(t) = C_{mn}\cos\sqrt{\frac{c}{\rho}\lambda_{mn}}t + C^*_{mn}\sin\sqrt{\frac{c}{\rho}\lambda_{mn}}t \tag{31}$$

Coupling (29) and (31) with (25) and rearranging the summation indices yields

$$w(x,y,t) = \sum_{m=1}^{\infty}\sum_{n=1}^{\infty}\left(A_{mn}\cos\sqrt{\frac{c}{\rho}\lambda_{mn}}t + A^*_{mn}\sin\sqrt{\frac{c}{\rho}\lambda_{mn}}t\right)\sin\frac{m\pi x}{a}\sin\frac{n\pi y}{b} \tag{32}$$

With the initial conditions (24) we have

$$A_{mn} = \frac{4}{ab}\int_0^a\int_0^b f(x,y)\sin\frac{m\pi x}{a}\sin\frac{n\pi y}{b}dxdy, \quad A^*_{mn} = \frac{4}{ab}\frac{1}{\sqrt{\frac{c}{\rho}\lambda_{mn}}}\int_0^a\int_0^b \sin\frac{m\pi x}{a}\sin\frac{n\pi y}{b}g(x,y)dxdy \tag{33}$$

6. Numerical examples

In the first case, a rectangular simply supported plate subjected to uniformly distributed load of $p(x,y) = 10^3$ N/m^2 is considered. The dimensions of the plate are specified as $a \times b \times h = 1\text{ m} \times 2\text{ m} \times 0.05\text{ m}$. The Young's modulus and Poisson's ratio are chosen as $E = 200$ GPa and $\nu = 0.3$, respectively. The PD horizon size is chosen as $\delta = 0.001$ m. The variation of displacement w along central x and y directions obtained by using PD and classical plate theory are shown in Fig. 3. It can be observed that a very good agreement is obtained between two approaches.

In the second example the same plate as in the previous case is considered except the distributed load is replaced by a concentrated load of 10^3 N in the central point. The concentrated load is achieved by invoking Dirac delta function such that $p(x,y) = -10^3\delta(x - a/2)\delta(y - b/2)$. Variation of displacement of central x and y directions obtained by PD and classical plate theory are illustrated in Fig. 4. A very good agreement is observed.

The third case aims to verify the validation of PD analytic solution for free vibrational condition. A simply supported plate with dimensions of $a \times b \times h = 1\text{ m} \times 1\text{ m} \times 0.05\text{ m}$ subjected to initial conditions of

$$f(x,y) = 0.01xy(x-a)(y-b), \quad g(x,y) = 10xy(x-a)(y-b)$$

is considered. The Young's modulus $E = 200$ GPa, the Poisson's ratio $\nu = 0.3$ and PD horizon size $\delta = 0.001$ m are chosen. It can be observed from Eq. (32) that the vibrational amplitude and frequencies depend upon

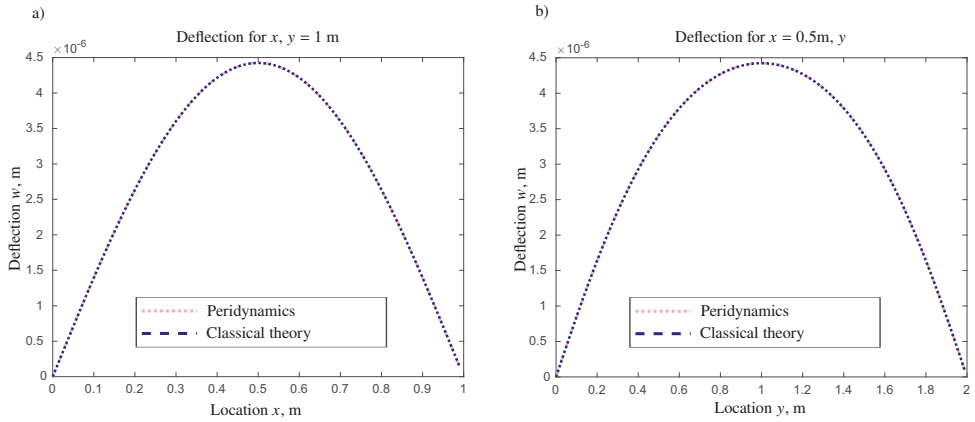

Fig. 3. Deflection vs coordinates of a simply supported plate under distributed load. a) For x, y = 1 m, b) for x = 0.5m, y

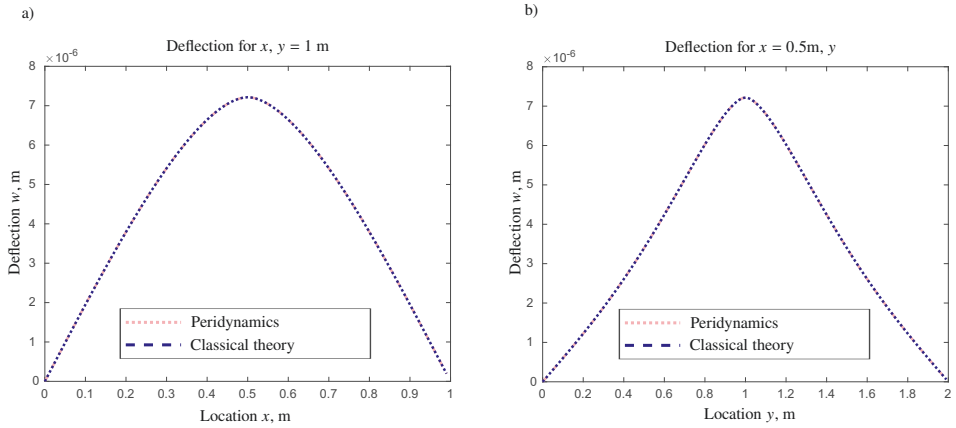

Fig. 4. Deflection vs coordinates of a simply supported plate under concentrated load. a) For x, y = 1 m, b) for x = 0.5m, y

the PD horizon size δ. In order to investigate the effect of the horizon size on dynamic behaviors, horizon sizes of δ = 1 mm, δ = 10 mm, δ = 50 mm and δ = 100 mm are taken into consideration. The vibrational trajectory of material point (0.5 m, 0.5 m) is tracked and illustrated in Fig. 5. PD solutions match well with those of the classical plate theory when horizon size is small. However, as the horizon size increase, PD results deviate from CPT results. This phenomena is expected since for large horizon size, nonlocality of PD starts to emerge and represent a behavior different from the classical one.

7. Conclusions

In this study, novel closed-form analytical solutions to equations of the PD Kirchhoff-type plate theory are presented. By the use of double trigonometric series representation of the deflection function with respect to the in-plane coordinates, general solutions for the static and dynamic cases are derived. For simply supported plates the coefficients in the series are found in a closed analytical form. For the dynamic case by the use of the variable separation the deflection is specified as a function of the time and the in-plane coordinates. Numerical examples are presented to illustrate and to compare results of PD with corresponding solutions

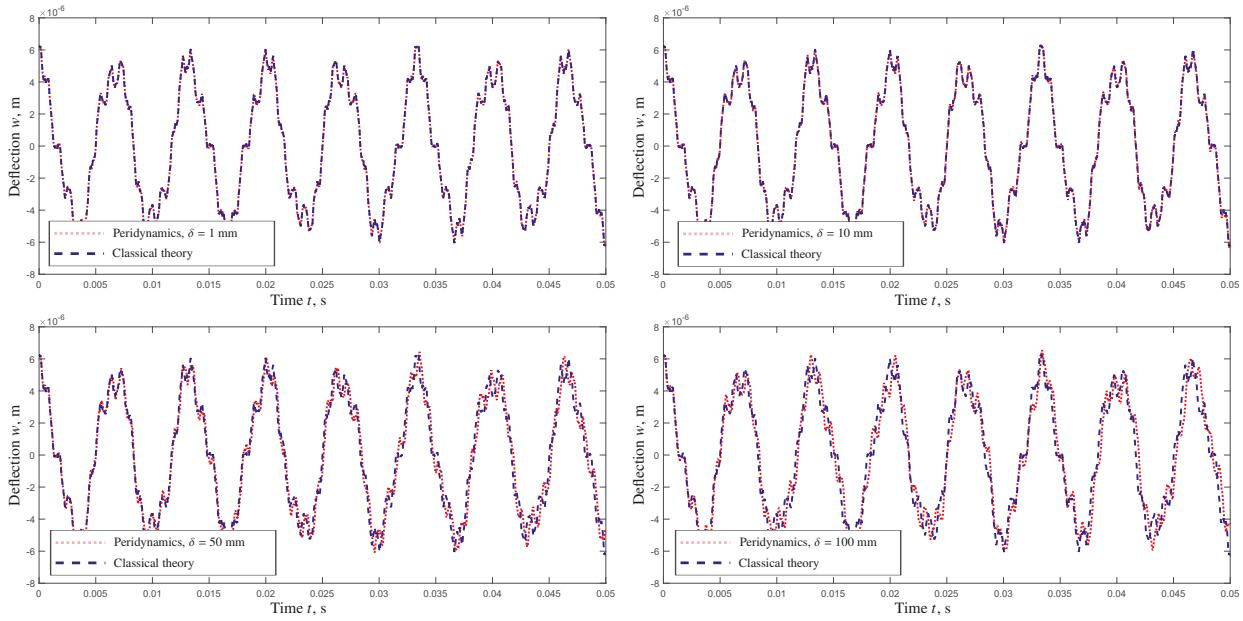

Fig. 5. Deflection vs time for a simply supported plate for different horizon sizes and $x = 0.5$ m, $y = 0.5$ m

to the classical plate equations. A very good agreement between these two different approaches is observed for the case of the small horizon sizes. This confirms the capability of the PD plate equations and derived closed form solutions.

References

[1] S. A. Silling, R. B. Lehoucq, Peridynamic theory of solid mechanics, Advances in applied mechanics 44 (2010) 73–168.

[2] K. Naumenko, M. Pander, M. Würkner, Damage patterns in float glass plates: Experiments and peridynamics analysis, Theoretical and Applied Fracture Mechanics 118 (2022) 103264.

[3] J. Mehrmashhadi, M. Bahadori, F. Bobaru, On validating peridynamic models and a phase-field model for dynamic brittle fracture in glass, Engineering Fracture Mechanics 240 (2020) 107355.

[4] Z. Yang, E. Oterkus, S. Oterkus, A state-based peridynamic formulation for functionally graded Euler-Bernoulli beams, CMES-Computer Modeling in Engineering and Sciences 124 (2020) 527–544.

[5] K. Naumenko, V. A. Eremeyev, A non-linear direct peridynamics plate theory, Composite Structures 279 (2022) 114728.

[6] C. T. Nguyen, S. Oterkus, Ordinary state-based peridynamics for geometrically nonlinear analysis of plates, Theoretical and Applied Fracture Mechanics 112 (2021) 102877.

[7] Z. Yang, B. Vazic, C. Diyaroglu, E. Oterkus, S. Oterkus, A Kirchhoff plate formulation in a state-based peridynamic framework, Mathematics and Mechanics of Solids 25 (2020) 727–738.

[8] S. R. Chowdhury, P. Roy, D. Roy, J. Reddy, A peridynamic theory for linear elastic shells, International Journal of Solids and Structures 84 (2016) 110–132.

[9] C. T. Nguyen, S. Oterkus, Peridynamics for the thermomechanical behavior of shell structures, Engineering Fracture Mechanics 219 (2019) 106623.

[10] S. P. Timoshenko, S. Woinowsky-Krieger, Theory of Plates and Shells, McGraw-Hill, New York, 1959.

[11] K. Naumenko, J. Altenbach, H. Altenbach, V. Naumenko, Closed and approximate analytical solutions for rectangular mindlin plates, Acta Mechanica 147 (2001) 153–172.

[12] Y. Mikata, Analytical solutions of peristatic and peridynamic problems for a 1D infinite rod, International Journal of Solids and Structures 49 (2012) 2887–2897.

[13] S. A. Silling, M. Zimmermann, R. Abeyaratne, Deformation of a peridynamic bar, Journal of Elasticity 73 (2003) 173–190.

[14] O. Weckner, R. Abeyaratne, The effect of long-range forces on the dynamics of a bar, Journal of the Mechanics and Physics of Solids 53 (2005) 705–728.